Automatic Detection of Choroidal Vascular Hyperpermeability Using Machine Learning Strategies

Deteção Automática de Hiperpermeabilidade Vascular Coroideia Utilizando Estratégias de *Machine Learning*

Pedro Carreira [1,*], João Salgueiro [2,*], Mariana Vaz [1], Margarida Brízido [1], Daniel Lopes [2], Diogo Cabral [1,3]

[1] Centro de Responsabilidade Integrada de Oftalmologia, Hospital Garcia de Orta, Almada, Portugal
[2] Instituto Superior Técnico, universidade de Lisboa, Lisboa, Portugal
[3] iNOVA4Health, NOVA Medical School I Faculdade de Ciências Médicas, Universidade NOVA de Lisboa, Lisboa, Portugal
* equal contribution

Recebido/Received: 2023-10-15 | **Aceite/Accepted:** 2024-05-28 | **Published online/Publicado online:** 2024-12-10 | **Published/Publicado:** 2025-06-30

DOI: https://doi.org/10.48560/rspo.33230

ABSTRACT

INTRODUCTION: Our purpose was to develop an artificial intelligence system capable of accurately predict choroidal vascular hyperpermeability (CVH) using swept-source optical coherence tomography (SS-OCT).

METHODS: This was a retrospective observational study conducted in healthy and CSC patients. All cases underwent ultra-widefield (UWF) indocyanine green angiography (ICGA) using a confocal scanning laser ophthalmoscopy (SLO) device and widefield (WF) SS-OCT. To segment the choroid in each individual B-scan, an automatic segmentation model was created and its performance was evaluated. Thickness maps were generated. Then, to predict the presence of choroidal hyperpermeability, based on the choroidal thickness maps, we developed an automatic classification model. To evaluate this classification model a validation dataset was used, superimposing the generated thickness maps with ICGA scans.

RESULTS: A total of 26 eyes from 13 CSC patients and 14 eyes from 7 healthy patients were included. In our analysis, the automatic segmentation model achieved a precision of 94.72%. The automatic hyperpermeability classification model based on SS-OCT had a false-positive rate of 0%, but a false-negative rate of 18.75%.

CONCLUSION: In the presence of a high clinical suspicion of CVH, the automated classification model for hyperpermeability based on SS-OCT has proven to be a useful diagnostic method. However, due to the rate of false negatives, in cases where clinical suspicion remains high and the model yields a negative result, it may be worth considering performing an ICGA.

KEYWORDS: Central Serous Chorioretinopathy; Machine Learning; Tomography, Optical Coherence.

RESUMO

INTRODUÇÃO: O nosso objetivo foi desenvolver um sistema de inteligência artificial capaz de prever com precisão a hiperpermeabilidade vascular coroideia (CVH) usando tomografia de

coerência ótica *swept-source* de campo alargado (SS-OCT).

MÉTODOS: Estudo observacional retrospetivo realizado em pacientes saudáveis e com coriorretinopatia serosa central (CSC). Todos os casos foram submetidos a angiografia de verde de indocianina de campo ultra-alargado (UWF ICGA) usando um dispositivo de oftalmoscopia laser de varredura confocal (SLO) e SS-OCT. Para segmentar a coroide, em cada modo B, foi desenvolvido um modelo de segmentação automática e a sua performance foi avaliada. Foram gerados mapas de espessura. Em seguida, para prever a presença de hiperpermeabilidade da coroide, com base nesses mapas, foi desenvolvido um modelo automático de classificação. Para avaliar este modelo de classificação, foi utilizado um conjunto de dados de validação, sobrepondo os mapas de espessura gerados com as imagens de ICGA.

RESULTADOS: Um total de 26 olhos de 13 pacientes com CSC e 14 olhos de 7 pacientes saudáveis foram incluídos neste estudo. O modelo de segmentação automática atingiu uma precisão de 94,72%. O modelo de classificação automática de hiperpermeabilidade com base em SS-OCT teve uma taxa de falsos positivos de 0%, mas uma taxa de falsos negativos de 18,75%.

CONCLUSÃO: Na presença de uma forte suspeita clínica de hiperpermeabilidade vascular coroideia, o modelo de classificação automática baseado em SS-OCT demonstrou ser um método de diagnóstico útil. No entanto, devido à taxa de falsos negativos, em casos em que a suspeita clínica permaneça alta e o modelo registe um resultado negativo, devemos considerar a realização de uma IGCA.

PALAVRAS-CHAVE: Aprendizagem Automática; Coriorretinopatia Serosa Central; Tomografia de Coerência Ótica.

INTRODUCTION

Traditional classification schemes for pachychoroid have often used subfoveal choroidal thickness to differentiate eyes with pachychoroid disease.[1] Eventually, the absolute thickness value seemed nonspecific enough for accurate classification, and other terms such as "pachyvessels," "focal choroidal thickening"," "thinning of the choriocapillaris and Sattler layers," and "RPE abnormalities over the pachyvessels" emerged to differentiate pathologic choroidal patterns in structural OCT.[2] However, the presence of these changes alone may not be sufficient to identify a diseased choroid, and identification of pachychoroid and pachychoroid disease in practice usually follows Potter Stweart's dictum "I know it when I see it".

Central serous chorioretinopathy (CSC) is the most prevalent clinical manifestation within the pachychoroid disease spectrum and is recognized primarily by the development of serous retinal detachment.[2] Identifying CSC biomarkers has been challenging, but recent advances in biomedical imaging techniques have led to breakthroughs.

Indocyanine green angiography (ICGA) is currently the gold standard to evaluate the choroidal vasculature.[3] ICGA allows the identification of delayed choroidal filling, choroidal vascular hyperpermeability and dilated choroidal vessels in patients with CSC.[4] However, ICGA is an invasive, time-consuming and expensive procedure, involving intravenous dye injection. Due to these challenges, there is growing interest in developing non-invasive and more time-efficient alternatives.

The development of optical coherence tomography (OCT) technology with the emergence of *swept-source* OCT (SS-OCT), improved depth imaging and enabled the acquisition of high-resolution volumetric cubes of the choroid, from which *en face* sections can be constructed.[1] Using SS-OCT, the choroid–scleral interface (CSI) can be delineated in most eyes, thus facilitating quantitative analysis of choroidal thickness.[5] The area of maximal choroidal thickness is likely to be of significance if it correlates spatially with the distribution of pachyvessels and with the hotspot of the disease.[6] Recently, Ramtohul *et al* have shown the ability of ultra-widefield SS-OCT (UW-OCT) to replicate some of the choroidal venous insufficiency features identified by ICGA.[6]

OCT can generate *en face* scans and choroidal thickness maps by processing the data from multiple B-scans. However, this process requires the segmentation of numerous B-scans, making manual segmentation impractical. Therefore, automatic image segmentation methods are essential for efficiently transforming OCT scans into clinically informative images.

Neural Networks (NNs) are potent tools in computer vision, especially in tasks like semantic segmentation, where they effectively emulate the neural behavior of the human brain. SegResNet is a type of NNs, frequently employed in image segmentation tasks.

Detecting choroidal venous overload (CVO) through imaging techniques can aid in the diagnosis of CVO-related diseases and guide decision-making in daily practice. This project aims to automatically classify generated thickness maps based on the presence of hyperpermeability points. The pipeline's objective is to take in an OCT scan and output a Boolean flag, indicating the suspected presence of

CVH, thus aiding in medical diagnosis and analysis. We aim to develop an artificial intelligence system capable of accurately detecting CVH using SS-OCT.

METHODS

This was a retrospective observational study that included healthy patients and patients diagnosed with CSC at Hospital Garcia de Orta from the practice of one retina specialist (DC), between June 2022 and September 2023. The study was conducted by the principles of the Declaration of Helsinki, written informed consent was obtained from each participant and IRB approval was obtained from Comissão de Ética para a Saúde do Hospital Garcia de Orta (Almada, Portugal).

For all cases and controls, comprehensive ophthalmic examination including best corrected visual acuity (BCVA) assessment, slit lamp examination, Goldmann applanation tonometry and fundus examination were performed.

CSC diagnosis was based on the clinical history, ophthalmoscopic examination, and retinal imaging using multimodal imaging (presence of serous retinal detachment on SS-OCT, typical dye leakage on FA, choroidal vascular hyperpermeability (CVH) on mid- to late-phase ICGA, focal or diffuse increased choroidal thickness and absence of macular neovascularization on SS-OCTA.[7]

We excluded patients with any ocular or systemic condition possibly affecting the diagnosis of CSC, including a history of ocular trauma, choroidal neovascularization, uveitis, retinal surgery, glaucoma filtration surgery, extreme axial lengths and/or refractive error inferior to - 6 or superior to + 3 diopters, pregnant women, and/or choroidal tumors.

All patients underwent UWF ICGA using a confocal scanning laser ophthalmoscopy (SLO) platform coupled with a widefield adapter of 163º (Mirante, Nidek Co. Ltd., Gamagori, Japan) or a SLO with Ultra-Widefield Angiography Module (Spectralis, Heidelberg Engineering, Germany). UWF ICGA images were acquired after intravenous administration of 0.2 mg/kg of indocyanine green at the early (up to 3 minutes after injection), middle (5 to 10 minutes), and late phases (10 to 20 minutes) of the angiogram.

SS-OCTA data was acquired using PLEX Elite 9000 SS-OCTA (Carl Zeiss Meditec, Inc., Dublin, CA, USA) with a scanning speed of 100 000 A-scans/s, lateral resolution of 20 µm, axial resolution of 6.3 µm, with a near-infrared illumination of 1040 - 1060 nm. Images with a quality index ≥ 7 were selected. WF OCT scans of 15 x 15 mm using a scanning speed of 200KHz were obtained.

WF OCT scans of 15 x 15 mm are composed of 834 individual scans with a width of 834 pixels. Due to poor quality of the scans at the edges, the first 75 and the last 75 images were excluded, leaving 684 images. The images were also cropped to a width of 684 pixels. Manual segmentation of all the 684 images would be unpractical, therefore an automatic segmentation model was created Fig. 1. To train the model, we used a dataset of 120 OCT B-scans that were manually segmented by a retinal specialist (DC). The split between validation/training was 80% - 20%. We compared 4 different architecture models (UNET, UNET++, DRUNET, SegResNet) with the ground truth (manual segmentation by DC). Due to hardware limitations, model size was restricted to a maximum of 3 layers.

All individual B-scans were then fed into the model. For each B-scan, the thickness was measured along the y-axis of the image. Each image produced an array with 684 thickness values. By composing these arrays of all the 684 images, a 684 x 684 thickness map was generated. We then converted the thickness value to a color gradient, with a maximum of 120 pixel, which corresponds to about 468 µm (~3.9 µm per pixel).

To access the performance of the segmentation model, we measured the Sorensen–Dice coefficient (more commonly referred as Dice), recall, pixel accuracy and precision, described by the following formulas (TP: true positives, FP: false positives, FN: false negatives, TN: true negatives):

$$Dice = \frac{2 \times TP}{(TP + FP) + (TP + FN)}$$

$$Recall = \frac{TP}{TP + FN}$$

$$Pixel\ Accuracy = \frac{TP + TN}{TP + TN + FN + FP + FN}$$

$$Precision = \frac{TP}{TP + FP}$$

To predict the presence of hyperpermeability spots in the choroid, we developed an automatic classification model, based on the ResNet-50 architecture, using the previously created choroidal thickness maps.

For training the model, individual thickness maps were collected, half with the presence of CVH and the other half without the presence of CVH. Data augmentation techniques such as flipping the image along the x- and y-axes and adding noise were used to augment the data set. The generated thickness maps were automatically classified by the model as having or not having CVH.

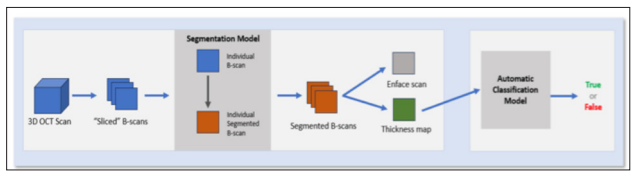

Figure 1. Graphical representation of the two sections in the proposed architecture.

To evaluate the classification model, a validation dataset of individual scans was used, superimposing the generated thickness maps with ICGA scans. ICGA and generated thickness maps were registered using the plugin landmark correspondences for Fiji (U. S. National Institutes of Health, Bethesda, Maryland) by selecting 6 corresponding points for each pair of images and employing a similarity algorithm. The areas of CVH on the ICGA were compared with the generated thickness maps.

RESULTS

A total of 26 eyes from 13 CSC patients and 14 eyes from 7 healthy patients, 12 men (60%) and 8 women (40%) were enrolled. The mean age was 52 ± 15 years (range, 36 to 83 years). All evaluated patients diagnosed with CSC had a disease duration longer than 6 months.

Regarding the automatic segmentation model, the dataset used to train the model was composed of 120 OCT B-scans images that were manually segmented by a retinal specialist. The validation/training split was 80% - 20%. The comparison of the 4 models studied with the ground truth (manual segmentation by DC) showed that SegResNet marginally obtained the best results out of the four architectures. Table 1 details the results obtained by each model in the previously mentioned metrics.

Thickness maps, Fig. 2, were generated using the best segmentation model, SegResNet, as shown in Table 1.

Regarding choroidal thickness values, mean thickness of the choroid in the group of CSC patients was 41.74 ± 4.43 µm and in the group of healthy patients was 45.09 ± 9.43 µm. There was no statistical difference between the two groups (p= 0.98).

Table 1. Choroidal segmentation results (%).

Model	Layers	Dice	Acc	Rec	Prec
UNET	512x256x128	93.81	99.04	94.12	93.77
	512x256	90.11	96.30	91.78	91.21
UNET++	512x256x128	93.98	99.05	94.12	94.07
	512x256	90.63	96.47	91.83	91.37
DRUNET	512x256x128	94.27	99.11	94.04	94.66
SegResNet	**512x256x128**	**94.36**	**99.14**	**94.19**	**94.72**

dice, acc: pixel accuracy, rec: recall, prec: precision.

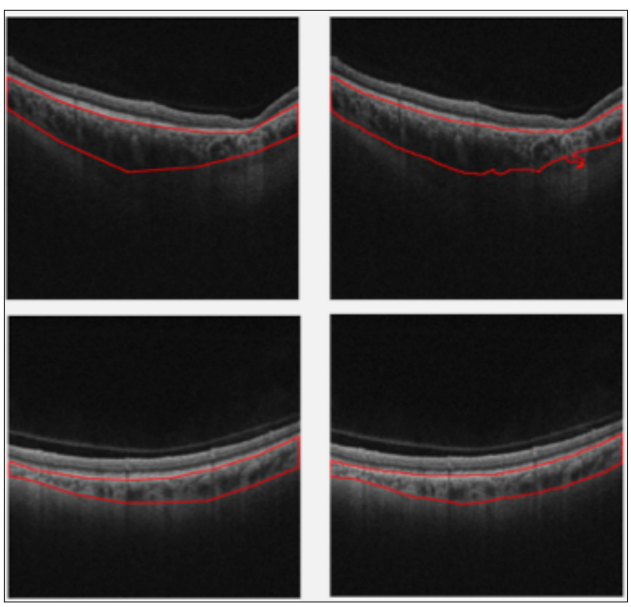

Figure 2. Swept-source optical coherence tomography B-scans segmented manually (left) and by the SegResNet architecture (right).

The thickness maps dataset was enlarged to a total of 130 images using data augmentation techniques. In the acquired dataset, approximately 70% of the scans with CVH showed affected areas coincident with areas of extreme thickening. Fig. 3 exemplifies such cases, in which CVH coincided with areas of abnormal thickening. On the other hand, Fig. 4 illustrates two cases of CSC with confirmed CVH; the one on the left has an abnormal thickness pattern but the one on the right shows an even distribution of thickness, very similar to what would be considered a healthy scan.

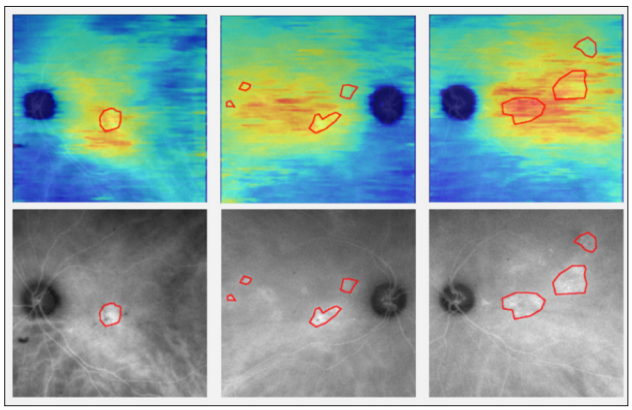

Figure 3. Thickness maps (top) and indocyanine green angiography (bottom) with the areas of choroidal hyperpermeability highlighted.

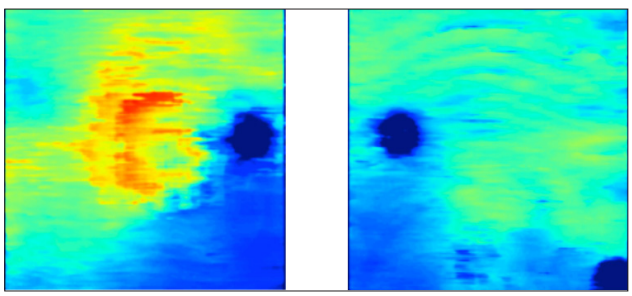

Figure 4. Two thickness maps of patients with CSC, both with the presence of choroidal vascular hyperpermeability confirmed by indocyanine green angiography.

Regarding the automatic hyperpermeability classification model, we used a validation dataset consisting of 30 individual thickness maps, 15 with CVH on ICGA (positive) and 15 without CVH on ICGA (negative). The model was able to predict 100% of negative scans as negative and 62.5% of positive scans as positive. The overall accuracy was 81.25%, with 0% of false positives (FP), but 18.75% of false negatives.

DISCUSSION

We herein describe AI-based algorithms for a three-dimensional segmentation of the choroid in widefield OCT that achieved a precision of 94.72% and for an automatic classification model for CVH that achieved a false-positive rate of 0%. To the best of our knowledge, this is the first study using AI that enables to infer choroidal changes typically observed using dye-contrast using non-invasive im-

aging. We believe that the findings described here add new information to our understanding of pachychoroid disease and open a pathway for the clinical application of widefield OCT to detect non-invasively distinctive pathologic features of pachycoroid disease.

The pathogenesis of pachychoroid disease itself remains unknown.[2] Previous studies have reported CVH to be present in >90% of eyes with CSC.[8] Eyes with CVH usually have increased choroidal thickness, but not all eyes with thick choroids exhibit CVH.[9] Although a complete understanding of choroidal vascular hyperpermeability remains controversial, recent works support that choroidal venous outflow abnormalities, i.e. choroidal venous overload, are an intrinsic phenomenon in CSC.[10]

Mid-late phase CVH in ICGA is a hallmark feature of CSC and has been considered a surrogate marker of choroidal venous congestion and a target for verteporfin photodynamic therapy. However, ICGA is an invasive, expensive, and time-consuming procedure that requires intravenous dye injection. Due to these challenges, there is growing interest in developing non-invasive and more time-efficient alternatives useful in any clinical setting.

Recently, Ramtohul *et al* showed that the ultra-widefield SS-OCT (UW-OCT) was able to replicate some of the choroidal venous insufficiency features identified by ICGA.[6] The authors used a semi-automated method based on proprietary Canon software to generate en face UWF OCT and thickness maps. The study demonstrated that SS-OCT is a plausible noninvasive alternative to ICGA by showing the correlation between CVH zones and increased choroidal thickness. Our results are partially consistent with the hypothesis put forward by Ramtohul *et al*[6] that the points of CVH coincide with areas of abnormal thickening, as shown in Fig. 3. However, we have also found cases with CVH on ICGA without associated choroidal thickening.

The literature on CSC indicates that abnormal choroidal thickness and abnormal choroidal patterns are potential biomarkers for CSC and thus a potential indicator for CVH. Therefore, the classification model in the proposed architecture intakes the output thickness map. Using the entire SS-OCT scan would be the optimal solution but due to the size of a scan (2 GB on average) and hardware limitations, we chose to use the thickness maps as input to the automatic classifier. The thickness maps produced were very reliable and provided important information about the patterns and overall areas of thickening.

In terms of choroidal segmentation, this study shows that the SegResNet architecture performs the best in all major evaluation metrics compared to other deep neural semantic segmentation models. Kugelman *et al* also used deep learning methods to determine the location of choroidal boundaries in a population of healthy individuals.[11] The results of their deep-learning methods were compared with manual boundary segmentation used as a ground-truth. In our model, we included a population with choroidal pathology and obtained similar results to Kugelman *et al*.[11] We consider this to be a strength of our study, as we studied patients with pachychroid disease which choroid is typically more difficult to segment.

Another important finding in this study was the automatic hyperpermeability classification model. The model showed high overall accuracy in the validation set (0% false positives) but it was only moderately able to identify a choroid without hyperpermeability points (18.75% false negatives). The moderately high number of FN seems to indicate that CSC and the presence of CVH are not always associated with an extremely abnormal pattern of choroidal thickness. In these cases, the model had difficulty providing a sufficiently accurate classification.

This hypothesis is further corroborated by a direct comparison between the mean choroidal thickness between the CSC group and the healthy group. The absence of a significant difference suggests that the ability of our automatic classification model for CVH is influenced by the pattern of choroidal thickness rather than by absolute choroidal thickness values.

These results show that thickened choroid per se does not necessarily mean pathologic consequences. In fact, the definition of pachychoroid-related disorders has shifted away from simply an abnormally thick choroid toward the morphological features of pathologic sequelae resulting from abnormally dilated choroid.[12] Eyes with pachychoroid disease may have normal subfoveal choroidal thickness, but exhibit an extrafoveal focus of increased choroidal thickness. The area of maximal choroidal thickness is likely to be of significance if it correlates spatially with the distribution of pathologically dilated vessels: pachyvessels and with the disease focus.[2]

In the presence of a high clinical suspicion of CVH, the automatic classification model for hyperpermeability based on SS-OCT has proven to be a useful diagnostic method. However, due to the rate of false negatives, in cases where clinical suspicion remains high and the model yields a negative result, it may be worth considering performing an ICGA.

The main strengths of this study are the high overall accuracy in the validation set (0% false positives) and the development of a noninvasive artificial intelligence system capable of accurately predicting choroidal vascular hyperpermeability in healthy and pathological choroids, which might be a putative game-changer application of AI-based algorithms to daily clinical practice.

Finally, some limitations of our study must be considered. First, the retrospective nature and relatively small sample size. Second, the need for software validation in different populations. Third, the ability of the algorithm to classify a choroid without hyperpermeability points needs to be improved, thus reducing the false-negative rate. Also, we acknowledge that further research is needed to clarify several areas of uncertainty, most notably why some eyes with thick choroids, large vessels and CVH show no evidence of RPE alterations or SRF (uncomplicated pachychoroid).[2]

In summary, we developed an automatic choroidal segmentation model that achieved 94.72% precision. The generated thickness maps were used to develop an automatic classification model for CVH. This model showed high overall accuracy in the validation set (0% false positive results) but was only moderately able to identify choroid without hyperpermeability points (18.75% false negative

results). We hope that this work will open new avenues for developments in artificial intelligence for ophthalmology that will be useful for decision making in clinical practice.

CONTRIBUTORSHIP STATEMENT / DECLARAÇÃO DE CONTRIBUIÇÃO:

JS, PC, DC e MV: Responsible for gathering the data.

PC, JS, DC e MB: Responsible for creating the manuscript.

DC, DL e MB: Supervised this project and contributed with their expertise to its conclusion.

All authors read and approved the final manuscript.

JS, PC, DC and MV: Responsável pela recolha dos dados.

PC, JS, DC and MB: Responsáveis pela criação do manuscrito.

DC, DL and MB: Supervisionaram este projeto e contribuíram com os seus conhecimentos para a sua conclusão.

Todos os autores leram e aprovaram o manuscrito final.

RESPONSABILIDADES ÉTICAS

Conflitos de Interesse: Os autores declaram a inexistência de conflitos de interesse na realização do presente trabalho.

Fontes de Financiamento: Não existiram fontes externas de financiamento para a realização deste artigo.

Confidencialidade dos Dados: Os autores declaram ter seguido os protocolos da sua instituição acerca da publicação dos dados de doentes.

Proteção de Pessoas e Animais: Os autores declaram que os procedimentos seguidos estavam de acordo com os regulamentos estabelecidos pelos responsáveis da Comissão de Investigação Clínica e Ética e de acordo com a Declaração de Helsínquia revista em 2013 e da Associação Médica Mundial.

Proveniência e Revisão por Pares: Não comissionado; revisão externa por pares.

ETHICAL DISCLOSURES

Conflicts of Interest: The authors have no conflicts of interest to declare.

Financing Support: This work has not received any contribution, grant or scholarship

Confidentiality of Data: The authors declare that they have followed the protocols of their work center on the publication of data from patients.

Protection of Human and Animal Subjects: The authors declare that the procedures followed were in accordance with the regulations of the relevant clinical research ethics committee and with those of the Code of Ethics of the World Medical Association (Declaration of Helsinki as revised in 2013).

Provenance and Peer Review: Not commissioned; externally peer reviewed.

REFERENCES

1. Dansingani KK, Balaratnasingam C, Naysan J, Bailey Freund K. En face imaging of pachychoroid spectrum disorders with swept-source optical coherence tomography. Retina. 2016;36:499-516. doi: 10.1097/IAE.0000000000000742.
2. Cheung CM, Lee WK, Koizumi H, Dansingani K, Lai TY, Freund KB. Pachychoroid disease. Eye. 2019;33:14-33. doi: 10.1038/s41433-018-0158-4. E
3. Yannuzzi LA. Indocyanine green angiography: A perspective on use in the clinical setting. Am J Ophthalmol. 2011;151:745-751.e1.
4. Hiroe T, Kishi S. Dilatation of asymmetric vortex vein in central serous chorioretinopathy. Ophthalmol Retina. 2018;2:152–61. doi: 10.1016/j.oret.2017.05.013.
5. Mrejen S, Spaide RF. Optical coherence tomography: imaging of the choroid and beyond. Surv Ophthalmol. 2013;58:387-429. doi: 10.1016/j.survophthal.2012.12.001.
6. Ramtohul P, Cabral D, Oh D, Galhoz D, Freund KB. En face Ultrawidefield OCT of the Vortex Vein System in Central Serous Chorioretinopathy. Ophthalmol Retina. 2023;7:346-53. doi: 10.1016/j.oret.2022.10.001.
7. van Dijk EH, Boon CJ. Serous business: Delineating the broad spectrum of diseases with subretinal fluid in the macula. Prog Retin Eye Res. 2021;84:100955. doi: 10.1016/j.preteyeres.2021.100955.
8. Giray Ersoz M, Arf S, Hocaoglu M. Indocyanine green angiography of pachychoroid pigment epitheliopathy. Retina. 2018;38:1668-74. doi: 10.1097/IAE.0000000000001773.
9. Hata M, Oishi A, Shimozono M, Mandai M, Nishida A, Kurimoto Y. Early changes in foveal thickness in eyes with central serous chorioretinopathy. Retina. 2013;33:296-301. doi: 10.1097/IAE.0b013e31826710a0.
10. Spaide RF, Gemmy Cheung CM, Matsumoto H, Kishi S, Boon CJF, van Dijk EHC, et al. Venous overload choroidopathy: A hypothetical framework for central serous chorioretinopathy and allied disorders. Prog Retin Eye Res. 2022;86:100973. doi: 10.1016/j.preteyeres.2021.100973.
11. Kugelman J, Alonso-Caneiro D, Read SA, Hamwood J, Vincent SJ, Chen FK, et al. Automatic choroidal segmentation in OCT images using supervised deep learning methods. Sci Rep. 2019;9:13298. doi: 10.1038/s41598-019-49816-4.
12. Lee WK, Baek J, Dansingani KK, Lee JH, Freund KB. Choroidal morphology in eyes with polypoidal choroidal vasculopathy and normal or subnormal subfoveal choroidal thickness. Retina. 2016;36 Suppl 1:S73-S82. doi: 10.1097/IAE.0000000000001346.

Corresponding Author/
Autor Correspondente:

Diogo Cabral
Centro de Responsabilidade Integrada de Oftalmologia, Hospital Garcia de Orta, E.P.E
Av. Torrado da Silva,
2805-267 Almada, Portugal
E-mail: diogo.cabral@hgo.min-saude.pt

ORCID: 0000-0003-1968-3561